

# Temperature-dependent transformation thermotics: From switchable thermal cloaks to macroscopic thermal diodes

Ying Li<sup>2</sup>, Xiangying Shen<sup>1</sup>, Zuhui Wu<sup>1</sup>, Junying Huang<sup>1</sup>,

Yixuan Chen<sup>1</sup>, Yushan Ni<sup>2</sup>, and Jiping Huang<sup>1,\*</sup>

<sup>1</sup>*Department of Physics, State Key Laboratory of Surface Physics,  
Key Laboratory of Micro and Nano Photonic Structures (Ministry of Education),  
and Collaborative Innovation Center of Advanced Microstructures,*

*Fudan University, Shanghai 200433, China*

<sup>2</sup>*Department of Mechanics and Engineering Science,*

*Fudan University, Shanghai 200433, China*

(Dated: October 30, 2015)

## Abstract

The macroscopic control of ubiquitous heat flow remains poorly explored due to the lack of a fundamental theoretical method. Here, by establishing temperature-dependent transformation thermotics for treating materials whose conductivity depends on temperature, we show analytical and simulation evidence for switchable thermal cloaking and a macroscopic thermal diode based on the cloaking. The latter allows heat flow in one direction but prohibits the flow in the opposite direction, which is also confirmed by our experiments. Our results suggest that the temperature-dependent transformation thermotics could be a fundamental theoretical method for achieving macroscopic heat rectification, and provide guidance both for macroscopic control of heat flow and for the design of the counterparts of switchable thermal cloaks or macroscopic thermal diodes in other fields like seismology, acoustics, electromagnetics, or matter waves.

PACS numbers: 81.05.Xj, 44.90.+c, 74.25.fc

Heat flow is a ubiquitous phenomenon in nature, and hence how to control the flow of heat at will is of particular importance for human life. Fortunately, the past years have witnessed the possibility of manipulating phononic [1–7] or electronic [8–11] heat conduction *at the nanoscale*, which provides a promising method to make use of heat flux. So far, significant progresses have been made, such as computation [3], information storage [4] and caloritronics [8, 9]. On the contrary, steering heat conduction *at the macroscale* is still far from being satisfactory [12], which prohibits macroscopic thermal rectification for diverse thermal management problems, e.g., efficient refrigerators, solar cells, and energy-saving buildings [13–15]. A reason behind the situation is due to the lack of a fundamental theoretical method.

In 2008, Fan *et al.* [16] adopted a coordinate transformation approach to propose a class of thermal metamaterial where heat is caused to flow around an “invisible” region at steady state, thus called *thermal cloaking*. The cloaking originates from the fact that the thermal conduction equation remains form-invariant under coordinate transformation. So far, the theoretical proposal of steady-state thermal cloaking [16] and its extensions (say, bifunctional cloaking of heat and electricity [17] or nonsteady-state thermal cloaking [18]) have been experimentally verified and developed [19–23]. The theoretical treatment based on coordinate transformation [16–18, 24–28], which is called *transformation thermotics (or transformation thermodynamics)*, has a potential to become a fundamental theoretical method for macroscopically manipulating heat flow at will.

However, in order to realize desired macroscopic thermal rectification, say, switchable thermal cloaking and macroscopic thermal diodes, the existing transformation thermotics [16–18] is not enough since it only holds for materials whose conductivity is independent of temperature (thus called *linear materials*). For instance, the desired thermal diode should conduct heat in one direction, but insulate the heat in the opposite direction. This is a kind of asymmetric behavior of heat current. For this purpose, nonlinear materials (whose conductivity relies on temperature) must be adopted. Actually, it is long known that for many materials, their thermal conductivities ( $\kappa$ ) vary with temperature ( $T$ ): (1)  $\kappa$  increases as  $T$  increases. Say, for noncrystalline solids, a series of experiments on glass [29] showed that at low temperature the thermal conductivity is proportional to  $T^{1.6} \sim T^{1.8}$ ; (2)  $\kappa$  increases as  $T$  decreases. For example, measurements on single crystals of silicon and germanium from 3 K to their melting point [30] showed that their thermal conductivity

decreases faster than  $1/T$ .

### Temperature-dependent transformation thermotics

Now we are in a position to establish a theory of transformation thermotics for treating nonlinear materials, thus called *temperature-dependent transformation thermotics*. The details of the theory are given in Part I of Ref. [36], which yield the key formula, Eq. (S8). This Eq. (S8) denotes that instead of constructing materials for a background whose thermal conductivity is  $T$ -dependent, we may apply a  $T$ -involved transformation to the original thermal conduction equation. This process allows us to design switchable thermal cloaks and then macroscopic thermal diodes. The former serve as an extension of the extensively investigated cloaks without switches [16–23, 31]; the latter are actually a useful application of the former in this work. We proceed as follows.

### Switchable thermal cloaks

*Design.*— A traditional thermal cloak can protect a central region from an external heat flux and permits the region to remain a constant temperature without disturbing the temperature distribution outside the cloak (Fig. 1). To achieve this cloaking effect, a simple radial stretch transformation of polar coordinates may be performed. As schematically shown in Fig. 1, the circular region with radius  $R_2$  is compressed to the annulus region with radius in-between  $R_1$  and  $R_2$ , and the geometrical transformation can be written as

$$r' = r \frac{R_2 - R_1}{R_2} + R_1, \quad (1)$$

where  $r \in [0, R_2]$  and  $r' \in [R_1, R_2]$ . Here  $r'$  is the radial coordinate in physical space.

In order to realize different responses to heat flow on the two sides of a thermal diode, we need two types of thermal cloaks: one functions at high temperature (hereafter indicated as type-A cloaks), the other works at low temperature (type-B cloaks). Unlike some previous proposed switchable electromagnetic cloaks [32–34], the switching effect should be triggered automatically by temperature changes. For this purpose, an idea is to modify Eq. (1) as

$$r' = r \frac{R_2 - \tilde{R}_1(T)}{R_2} + \tilde{R}_1(T), \quad (2)$$

where  $\tilde{R}_1(T) = R_1[1 - (1 + e^{\beta(T-T_c)})^{-1}]$  for type-A cloaks and  $\tilde{R}_1(T) = R_1/(1 + e^{\beta(T-T_c)})$  for type-B cloaks. Here  $T_c$  is a critical temperature around which the cloak is switched on or off, and  $\beta$  is a scaling coefficient which is set to be  $2.5 \text{ K}^{-1}$  in this work.

So far, for obtaining thermal cloaks with switching phenomena, we need to combine Eq. (2) and Eq. (S8). As a result, for the area with radius  $r' \in [R_1, R_2]$  in Fig. 1, we achieve the thermal conductivities in polar coordinates,  $\text{diag}[\tilde{\kappa}_r(T), \tilde{\kappa}_\theta(T)]$ , as

$$\tilde{\kappa}_r(T) = \kappa_0 \frac{r' - \tilde{R}_1(T)}{r'}, \quad \tilde{\kappa}_\theta(T) = \kappa_0 \frac{r'}{r' - \tilde{R}_1(T)}. \quad (3)$$

Here  $\kappa_0$  represents the  $T$ -independent thermal conductivity of the background.

*Finite-element simulations.*— Then we perform finite element simulations based on the commercial software COMSOL Multiphysics. A thermal cloak with  $R_1 = 1$  cm and  $R_2 = 2$  cm is set in a box with size  $8 \text{ cm} \times 7 \text{ cm}$  as shown in Fig. 2. Heat diffuses from the left boundary with high temperature  $T_H$  to the right boundary with low temperature  $T_L$ . Meanwhile, the upper and lower boundaries of the simulation box are thermally isolated.

The simulation results of a type-A cloak are shown in Fig. 2(a,b). In Fig. 2(a), at high temperature ( $T = 340 \text{ K} \sim 360 \text{ K}$ ), we observe that the cloak is functioning and thermally hiding the object located at the central region with radius  $R_1$ . However, when the environment is changed to low temperature ( $T = 300 \text{ K} \sim 320 \text{ K}$ ), the cloak is turned off. That is, the temperature distribution outside the object is distorted, just as the cloak (located between  $R_1$  and  $R_2$ ) is absent. Owing to the antisymmetry between type-A and type-B cloaks, the type-B cloaks exhibit the behavior similar to Fig. 2(a,b), but switching on (or off) at low (or high) temperature.

*Theoretical realization based on the effective medium theory.*— The materials designed according to Eq. (3) is anisotropic and inhomogeneous, which is difficult to be realized in experiments. In fact, for constructing such materials, we can simply utilize alternating layers of two homogeneous isotropic sub-layers with thicknesses  $d_1$  and  $d_2$  and conductivities  $\kappa_a$  and  $\kappa_b$ . For simplification, in this work, we set  $d_1 = d_2$ . According to the theoretical analysis and effective medium theory (EMT) [17–19, 31, 35], the conductivities of two sub-layers should satisfy  $\kappa_a \kappa_b \approx \kappa_0^2$  for a traditional cloak. In order to endue conventional cloaks with the switching effect, some mathematical operations must be carried out on  $\kappa_a$  and  $\kappa_b$  in the way analogous to what we did on  $\tilde{R}_1(T)$ . Therefore, we obtain  $\kappa_1(T)$  and  $\kappa_2(T)$  as the new temperature-dependent thermal conductivities of the sub-layers,

$$\kappa_1(T) = \kappa_a + \frac{\kappa_0 - \kappa_a}{1 + e^{\beta(T-T_C)}}, \quad \kappa_2(T) = \kappa_b - \frac{\kappa_b - \kappa_0}{1 + e^{\beta(T-T_C)}}. \quad (4)$$

The two expressions yield:  $\kappa_1(T) \rightarrow \kappa_a$  and  $\kappa_2(T) \rightarrow \kappa_b$  when  $T \gg T_C$ ;  $\kappa_1(T) \rightarrow \kappa_0$  and  $\kappa_2(T) \rightarrow \kappa_0$  as  $T \ll T_C$ . (The detailed dependence of  $\kappa_1(T)$  and  $\kappa_2(T)$  on temperature

is displayed in Fig. S3 of Part III of Ref. [36].) That is, the cloaking effect is switched on (or off) for high (or low) temperature environment  $T \gg T_C$  (or  $T \ll T_C$ ). Eq. (4) offers a convenient tool to help experimentally realize our theoretical design of Eq. (3). Next, we plot Fig. 2(c,d), which shows the simulation results of 10 alternating layers for constructing type-A cloaks. Evidently, Fig. 2(c,d) displays the switching phenomenon similar to Fig. 2(a,b). The procedure holds the same for achieving type-B cloaks.

### Macro thermal diode

*Design.*— The above thermal cloaking may help to design a kind of macroscopic thermal diodes. As shown in Fig. 3(a), the diode device contains Regions I, II and III: Region I (II) is a segment of the type-A (type-B) cloak, and Region III is a thermal conductor. Compared with a full system, the cloaking effect still exists in our diode but is not perfect. There will be a small amount of heat flux conducting through the central region for the insulating case. However, the truncation of a whole cloak is necessary to separate the type-A part and the type-B part. The antisymmetry of type-A and type-B cloaks is expected to cause different behaviors of heat conducting from the two opposite directions. The transformation plays an important role in introducing anisotropic effect to the structure, which guides the heat flux to the boundaries to enhance the thermal insulating effect.

*Finite-element simulations.*— Then we perform finite element simulations. Fig. 3(c,d) shows the simulation results of the device, which helps to insulate heat from right to left but conduct the heat from left to right. That is, the behavior of diode can be achieved indeed due to the antisymmetry of type-A and type-B cloaks (namely, Region I and Region II). Moreover, for different temperature biases (obtained by subtracting the temperature at the left boundary from that at the right boundary),  $\Delta T$ , we also calculate the total heat current  $J$  by integrating the  $x$  component of heat flux across the line  $x = 0$ ; see Fig. 3(b). The device displays a significant rectifying effect, which has a maximum rectification ratio of 30 for the current parameter set.

*Experimental realization based on the effective medium theory.*— In order to realize such a macroscopic thermal diode, we can also adopt the EMT. As discussed above, the switchable thermal cloak can be constructed with alternating layers. The thermal conductivities of the sub-layers are required to be sensitive to the temperature change around the critical point. This kind of behaviors can be found in the phase transitions of some materials [37–39]. However, inspired by the spirit of metamaterials (yielding novel functions by assembling

conventional materials into specific structures), we manage to realize the macroscopic thermal diode with materials of constant conductivities. Our method is that instead of directly resorting to the transitions of materials' physical properties, we use the structural transition to trigger the switching effect. According to the demands of our design, the geometrical configuration of the device should change rapidly as temperature varies. Fortunately, we found that the shape-memory alloy (SMA) [40] may be able to help. As shown in the schematic diagrams of our design [see Fig. 4(a) and (b); more details of our experiment can be found in Part II of Ref. [36]], the sub-layers of the cloak segments are coppers and expanded-polystyrene (EPS). Around the critical temperature, the deformations of the SMA slices drive the copper slices to connect or disconnect the copper layers. The connection and disconnection can be equivalently regarded as transitions of the local thermal conductivities. Thus a temperature-dependent thermal metamaterial is realized with materials of constant thermal conductivities (a whole switchable thermal cloak can also be built with the same method). The experimental results are shown in Fig. 4(c) and (d). Fig. 4(c) displays the temperature distribution within the central region, which is almost constant. That is, in this case, heat almost cannot flow through this central region. Thus, Fig. 4(c) corresponds to the insulating case of the diode. In contrast, Fig. 4(d) represents the conducting case of the diode. This is because Fig. 4(d) shows a significant temperature gradient within the central region. Also, the temperature distribution appears to be horizontal. As a result, we can conclude that an evident heat flow comes to appear within the central region of Fig. 4(d).

## Conclusions

We have established a theory of temperature-dependent transformation thermotics for dealing with thermal materials whose conductivity is temperature-dependent. The theory serves as a fundamental theoretical method for designing switchable thermal cloaking. We have also shown that the switchable thermal cloaks can be employed for achieving a macroscopic thermal diode, which has also been experimentally realized by assembling homogeneous and isotropic materials according to the design based on the EMT (effective medium theory). The diode has plenty of potential applications related to heat preservation, heat dissipation, or even heat illusion [41, 42] in many areas like efficient refrigerators, solar cells, energy-saving buildings, and military camouflage. Thus, by using temperature-dependent transformation thermotics to tailor nonlinear effects appropriately, it becomes possible to achieve desired thermal metamaterials with diverse capacities for macroscopic thermal rec-

tification. On the same footing, our consideration (for cloaks and diodes) adopted in this work can be extended to obtain the counterparts of both switchable thermal cloaks and macroscopic thermal diodes in other fields like seismology, acoustics, electromagnetics, or matter waves.

*Acknowledgement.* We acknowledge the financial support by the National Natural Science Foundation of China under Grants No. 11222544 and No. 1157209 (Y.L. and Y.N.), by the Fok Ying Tung Education Foundation under Grant No. 131008, by the Program for New Century Excellent Talents in University (NCET-12-0121), and by the CNKBRSF under Grant No. 2011CB922004.

Y.L. and X.S. contributed equally to this work.

---

\* Electronic address: jphuang@fudan.edu.cn.

- [1] B. Li, L. Wang, and G. Casati, *Phys. Rev. Lett.* **93**, 184301 (2004).
- [2] C. W. Chang, D. Okawa, A. Majumdar, and A. Zettl, *Science* **314**, 1121 (2006).
- [3] L. Wang and B. Li, *Phys. Rev. Lett.* **99**, 177208 (2007).
- [4] L. Wang and B. Li, *Phys. Rev. Lett.* **101**, 267203 (2008).
- [5] N. Li, J. Ren, L. Wang, G. Zhang, P. Hanggi, and B. Li, *Rev. Mod. Phys.* **84**, 1045 (2012).
- [6] M. Maldovan, *Nature* **503**, 209 (2013).
- [7] Z. Chen, C. Wong, S. Lubner, S. Yee, J. Miller, W. Jang, C. Hardin, A. Fong, J. E. Garay, and C. Dames, *Nature Communications* **5**, 5446 (2014).
- [8] F. Giazotto and M. J. Martínez-Pérez, *Nature* **492**, 401 (2012).
- [9] M. J. Martínez-Pérez and F. Giazotto, *Nature Communications* **5**, 3579 (2014).
- [10] A. Fornieri, M. J. Martínez-Pérez, and F. Giazotto, *Appl. Phys. Lett.* **104**, 183108 (2014).
- [11] M. J. Martínez-Pérez, A. Fornieri, and F. Giazotto, *Nature Nanotech.* **10**, 303 (2015).
- [12] Y. Wang, A. Vallabhaneni, J. Hu, B. Qiu, Y. P. Chen, and X. Ruan, *Nano Lett.* **14**, 592 (2014).
- [13] W. Kobayashi, Y. Teraoka, and I. Terasaki, *Appl. Phys. Lett.* **95**, 171905 (2009).
- [14] D. Go and M. Sen, *J. Heat Trans.* **132**, 124502 (2010).
- [15] W. Kobayashi, D. Sawaki, T. Omura, T. Katsufuji, Y. Moritomo, and I. Terasaki, *Appl. Phys. Express* **5**, 027302 (2012).

- [16] C. Z. Fan, Y. Gao, and J. P. Huang, *Appl. Phys. Lett.* **92**, 251907 (2008).
- [17] J. Y. Li, Y. Gao, and J. P. Huang, *J. Appl. Phys.* **108**, 074504 (2010).
- [18] S. Guenneau, C. Amra, and D. Veynante, *Optics Express* **20**, 8207 (2012).
- [19] S. Narayana and Y. Sato, *Phys. Rev. Lett.* **108**, 214303 (2012).
- [20] R. Schittny, M. Kadic, S. Guenneau, and M. Wegener, *Phys. Rev. Lett.* **110**, 195901 (2013).
- [21] H. Xu, X. Shi, F. Gao, H. Sun, and B. Zhang, *Phys. Rev. Lett.* **112**, 054301 (2014).
- [22] T. Han, X. Bai, D. Gao, J. T. L. Thong, B. Li, and C.-W. Qiu, *Phys. Rev. Lett.* **112**, 054302 (2014).
- [23] Y. Ma, Y. Liu, M. Raza, Y. Wang, and S. He, *Phys. Rev. Lett.* **113**, 205501 (2014).
- [24] U. Leonhardt, *Science* **312**, 1777 (2006).
- [25] J. B. Pendry, D. Schurig, and D. R. Smith, *Science* **312**, 1780 (2006).
- [26] H. Chen, C. T. Chan, and P. Sheng, *Nature Materials* **9**, 387 (2010).
- [27] N. Landy and D. R. Smith, *Nature Materials* **12**, 25 (2013).
- [28] M. Kadic, T. Bückmann, R. Schittny, and Martin Wegener, *Rep. Prog. Phys.* **76**, 126501 (2013).
- [29] R. C. Zeller and R. O. Pohl, *Phys. Rev. B* **4**, 2029 (1971).
- [30] C. J. Glassbrenner and G. A. Slack, *Phys. Rev.* **134**, A1058 (1964).
- [31] T. Han, T. Yuan, B. Li, and C. Qiu, *Scientific Reports* **3**, 1593 (2013).
- [32] P. Y. Chen and A. Alù, *ACS Nano* **5**, 5855 (2011).
- [33] W. Zhang, W. M. Zhu, H. Cai, M. J. Tsai, G. Lo, D. P. Tsai, H. Tanoto, J. Teng, X. Zhang, D. Kwong, and A. Liu, *IEEE J. Sel. Top. Quant.* **19**, 4700306 (2013).
- [34] R. F. Wang, Z. L. Mei, X. Y. Yang, X. Ma, and T. J. Cui, *Phys. Rev. B* **89**, 165108 (2014).
- [35] J. P. Huang and K. W. Yu, *Phys. Rep.* **431**, 87 (2006).
- [36] See Supplemental Material at <http://link.aps.org/> for (Part I) temperature-dependent transformation thermotics, (Part II) our experimental demonstration of the macroscopic thermal diode, and (Part III) the temperature dependence of  $\kappa_1$  and  $\kappa_2$ .
- [37] D. Oh, C. Ko, S. Ramanathan, and D. G. Cahill, *Appl. Phys. Lett.* **96**, 151906 (2010).
- [38] R. Zheng, J. Gao, J. Wang, and G. Chen, *Nat. Commun.* **2**, 289 (2011).
- [39] K. S. Siegert, F. R. L. Lange, E. R. Sittner, H. Volker, C. Schlockermann, T. Siegrist, and M. Wuttig, *Rep. Prog. Phys.* **78**, 013001 (2015).
- [40] T. Omori and R. Kainuma, *Nature* **502**, 7469 (2013).



- [41] T. C. Han, X. Bai, J. T. L. Thong, B. W. Li, and C. W. Qiu, *Adv. Mat.* **26**, 1731 (2014).
- [42] N. Q. Zhu, X. Y. Shen, and J. P. Huang, *AIP Advances* **5**, 053401 (2015).

Fig. 1 (color online). Schematic graph depicting a thermal cloak between radius  $R_1$  and  $R_2$ . Red lines with arrows denote the flow of heat: the cloak does not disturb the heat flow at the region with radius larger than  $R_2$ ; the heat flux cannot enter the central region with radius smaller than  $R_1$ .

Fig. 2 (color online). Switchable thermal cloaks obtained by two-dimensional finite-element simulations: (a,c) switch on for the temperature above 340 K and (b,d) switch off for the temperature below 320 K. The color surface denotes the distribution of temperature, where isothermal lines are indicated; heat diffuses from left to right; the upper and lower boundaries are thermal insulation. (a) and (b) show the results of thermal conductivities calculated according to Eq. (3); (c) and (d) show the results of 10 alternating layers of two sub-layers with  $\kappa_1(T)$  and  $\kappa_2(T)$  given by Eq. (4) (EMT). In (a-d), an object with thermal conductivity 0.01 W/mK is set in the central region with radius  $R_1$ . Parameters:  $\kappa_0 = 1$  W/mK,  $\kappa_a = 0.1$  W/mK,  $\kappa_b = 10$  W/mK,  $R_1 = 1$  cm,  $R_2 = 2$  cm, and  $T_c = 330$  K.

Fig. 3 (color online). (a) Sketch of a thermal diode, which is the rectangular area enclosed by the solid black lines. The blurred area outside is a reference and actually does not exist in the design. I, II, and III represent three regions, respectively. Here the arrows indicate the direction of heat flow; the length of arrows represents the amount of heat flux: the heat flux transferred from right to left (upper panel: the insulating case) is much smaller than that from left to right (lower panel: the conducting case). (b) Heat current  $J$  versus temperature bias  $\Delta T$ . (c,d) Thermal diode obtained by two-dimensional finite-element simulations: (c) the insulating case and (d) the conducting case. The color surface denotes the distribution of temperature; white arrows represent the direction of heat flow; the length of white arrows indicates the amount of heat flux; the upper and lower boundaries are thermal insulation. Thermal conductivities are calculated according to Eq. (3); an object with thermal conductivity 10 W/mK is set in the central region with radius  $R_1$ . Parameters:  $\kappa_0 = 1$  W/mK,  $R_1 = 3.6$  cm,  $R_2 = 4$  cm, and  $T_c = 330$  K.

Fig. 4 (color online). (a,b) Scheme of experimental demonstration of the macroscopic thermal diode: (a) insulating case and (b) conducting case. Both the copper-made concentric layered structure and the central copper plate (both displayed in orange) are placed on an expanded-polystyrene (EPS) plate which is not shown for clarity. The left and right sides of the diode are stuck in water to have constant temperature boundary conditions. (a) When cold water is filled in the left container (light blue) and hot water the right container

(pale red), the bimetallic strips of SMA and copper (white) warp up and the device blocks heat from right to left. (b) When the two containers swap their locations, the bimetallic strips (white) flatten and the device conducts heat from left to right. (c,d) Experimentally measured temperature distribution of the device: (c) insulating case and (d) conducting case.

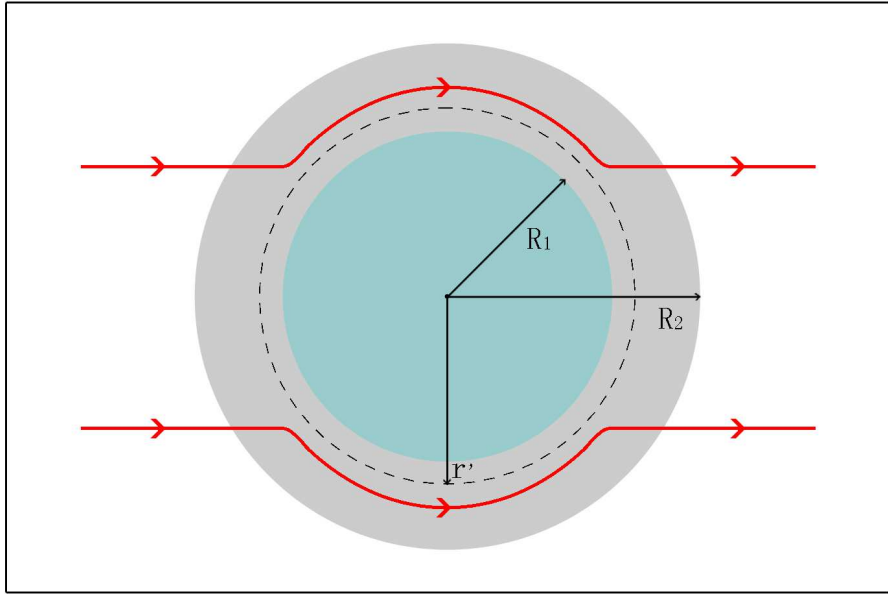


FIG. 1: /Li, Shen, Wu, Huang, Chen, Ni, and Huang

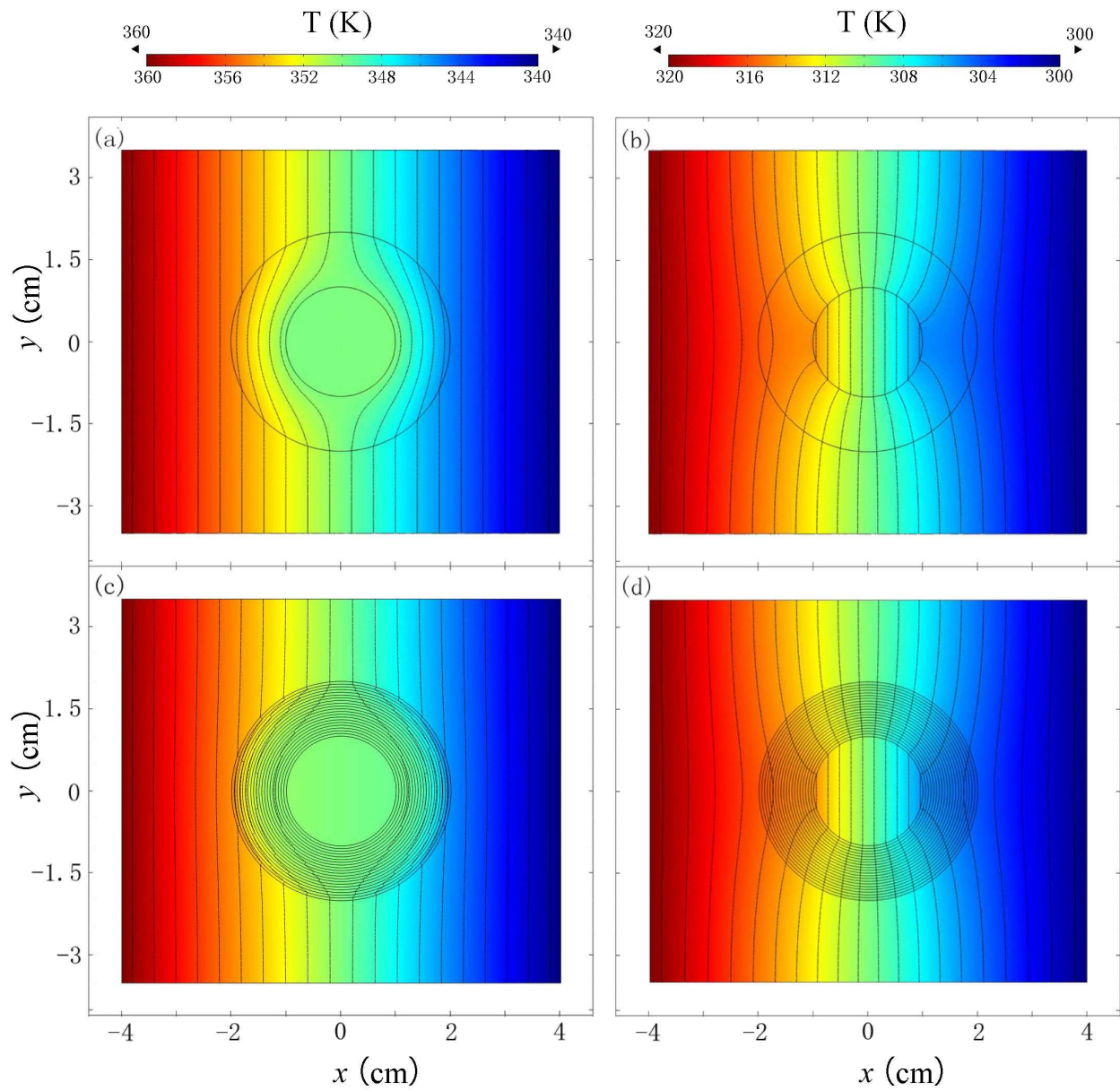


FIG. 2: /Li, Shen, Wu, Huang, Chen, Ni, and Huang

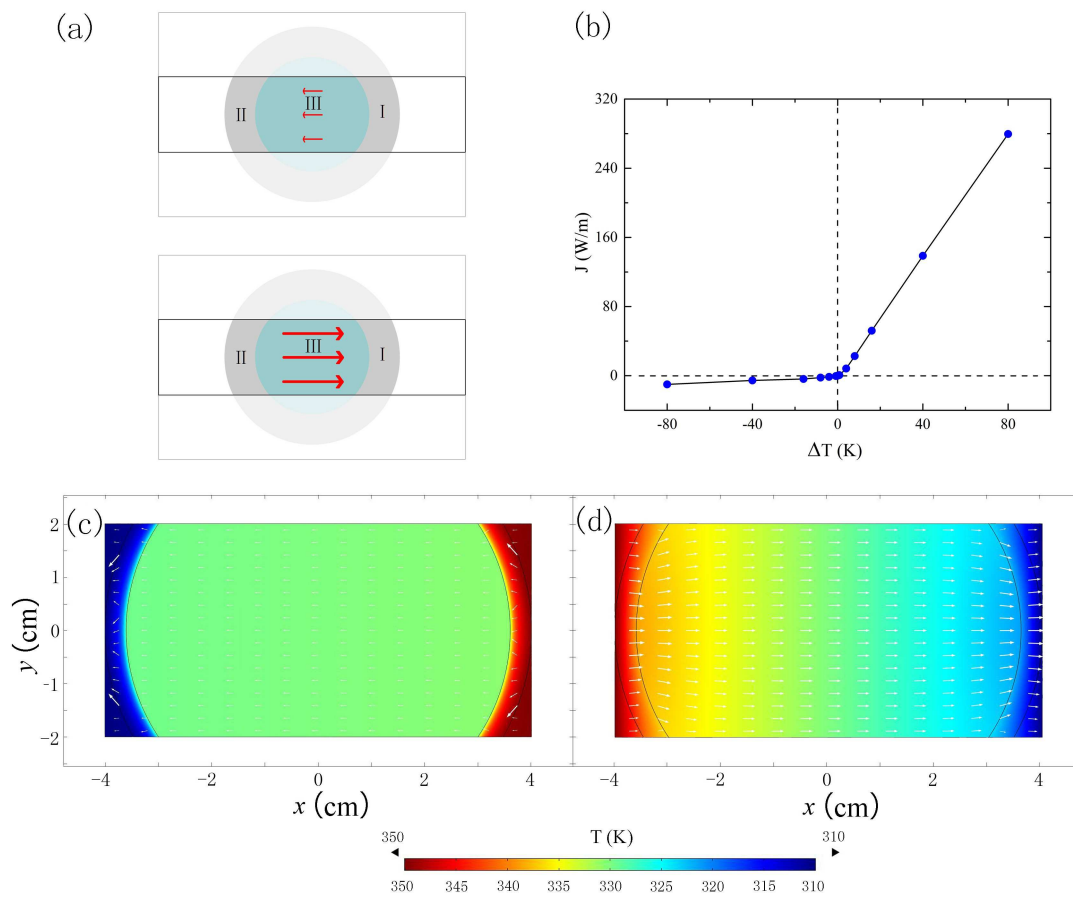


FIG. 3: /Li, Shen, Wu, Huang, Chen, Ni, and Huang

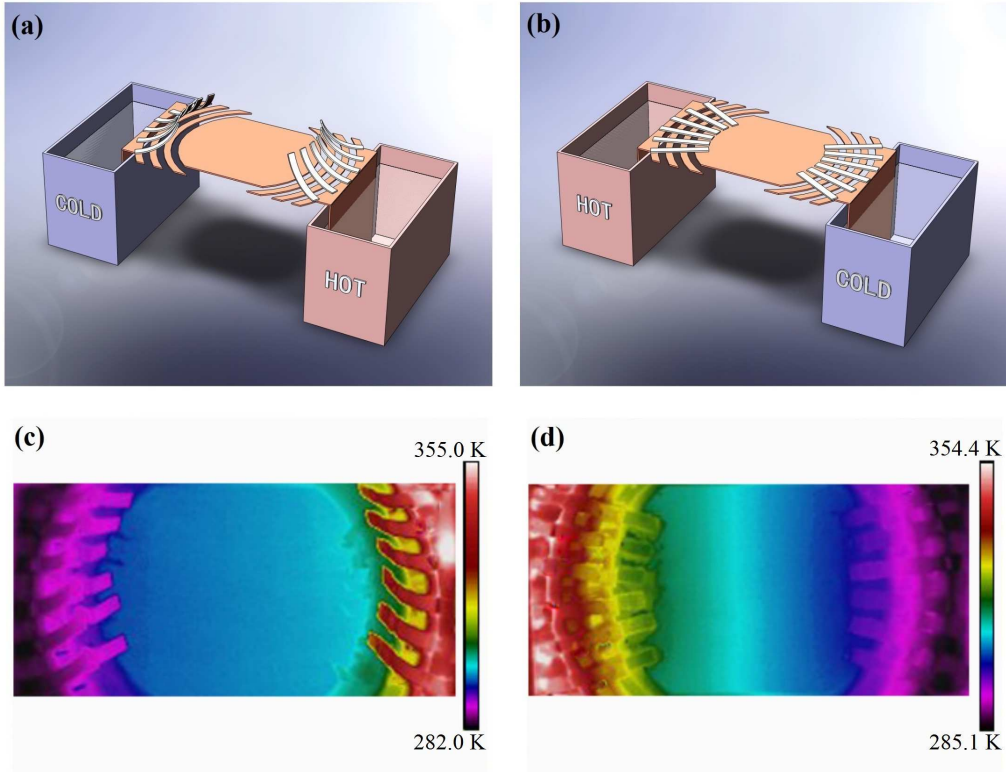


FIG. 4: /Li, Shen, Wu, Huang, Chen, Ni, and Huang